

Thermally activated relaxation of shear stress in solid ^4He confined in aerogel

A. Rabbani and J. R. Beamish

Department of Physics, University of Alberta, Edmonton, Alberta, Canada, T6G 2E1

(Received 26 May 2011; revised manuscript received 29 July 2011; published 13 September 2011)

Torsional oscillator (TO) experiments on ^4He show supersolid behavior that appears to be associated with disorder. However, confining helium in the pores of an aerogel does not enhance the supersolid decoupling, even though x-ray measurements confirm that the crystals are highly disordered. Solid helium's shear modulus also shows anomalous behavior below 200 mK, stiffening as mobile dislocations are pinned by ^3He impurities at low temperatures. A highly porous material such as aerogel should also provide effective pinning sites for dislocations. We have made shear modulus measurements on solid ^4He grown in a 95% porosity aerogel. We see large modulus decreases as the samples are warmed but these occur at much higher temperatures and over a broader range than in bulk ^4He . The frequency dependence of the modulus and dissipation are consistent with a thermally activated process. The activation energy is approximately 16 K and may be associated with vacancy motion.

DOI: [10.1103/PhysRevB.84.094509](https://doi.org/10.1103/PhysRevB.84.094509)

PACS number(s): 67.80.bd, 67.80.de, 67.80.dj

I. INTRODUCTION

When a torsional oscillator is filled with solid ^4He and cooled, its frequency increases at temperatures below about 200 mK, suggesting that a fraction of the solid decouples from the oscillator, the “nonclassical rotational inertia” (NCRI) that would characterize a supersolid.^{1,2} The NCRI fraction decreases at large oscillation amplitudes, behavior that has been interpreted in terms of a supersolid critical velocity of about 10 $\mu\text{m}/\text{second}$. The NCRI varies over a wide range (0.02% to 15%) in different oscillators and depends on crystal history. For example, polycrystals grown at constant density (“blocked capillary” growth) usually have larger NCRI (and higher onset temperatures) than single crystals grown at constant pressure and the NCRI often changes when a helium crystal is subsequently annealed^{3,4} or plastically deformed.⁵ This implies that crystal defects are involved in the TO behavior, a conclusion consistent with the path-integral Monte Carlo simulations, which find that superflow is possible along some dislocations and grain boundaries but not in perfect crystals.^{6,7} Also, the onset temperature of the TO anomaly depends strongly on ^3He impurity concentration, decreasing from about 200 mK in commercial ^4He (containing about 300 ppb ^3He) to 75 mK in isotopically purified ^4He (containing about 1 ppb ^3He). It is difficult to understand how such small impurity concentrations could have such large effects unless the behavior involves lower dimensional defects where impurities can accumulate.

Measurements^{8,9} of the elastic shear modulus μ of solid ^4He show a remarkable increase (of order 10%) in the same temperature range as the TO frequency increase. The onsets of both the shear modulus and TO anomalies are accompanied by dissipation peaks. The modulus anomaly has the same dependence on temperature, drive amplitude and ^3He concentration as the NCRI seen in TO experiments—the two phenomena are clearly related. The elastic measurements have been extended over a wide frequency range (from 0.5 Hz to above 8 kHz) and show that the anomaly shifts to lower temperature as the frequency decreases. The frequency and temperature dependence of the shear modulus and dissipation

can be described¹⁰ in terms of a thermally activated relaxation process with a broad distribution of activation energies around an average value of 0.7 K. Torsional oscillator measurements (in a TO with two modes at 493 and 1164 Hz) show similar behavior,¹¹ with an activation energy of about 0.4 K.

The shear modulus changes have a natural interpretation in terms of dislocation motion and pinning. Between pinning points they respond to shear stresses by “gliding” over the lattice's Peierls barrier. At high temperatures, dislocations are pinned only at their intersections (a distance L apart). The strain associated with their motion reduces the crystal's intrinsic shear modulus by an amount proportional to ΔL^2 (where Δ is the dislocation density). At low temperatures, ^3He impurities are bound to dislocations, further pinning them, which reduces L and restores the larger intrinsic shear modulus of the ^4He crystal. The unbinding of ^3He impurities as the temperature is raised is responsible for the observed modulus changes. Annealing and deformation of ^4He crystals both affect the magnitude of the modulus change, as expected when dislocations are eliminated or added. However, it is only the high-temperature behavior that changes—the low-temperature modulus is unaffected,⁹ as expected if all dislocations are pinned at the lowest temperatures.

In a recent experiment, a ^4He crystal was plastically deformed in the annular gap of a specially designed torsional oscillator.⁵ If the increase in TO frequency reflects the decoupling of a supersolid fraction (NCRI) associated with crystal defects, then plastic deformation (which increases defect densities) would be expected to raise the TO frequency at low temperatures but not to affect the high-temperature behavior in the normal state. However, the behavior at the lowest temperature was unaffected by deformation. Instead, the high-temperature TO frequency decreased after the deformation. This behavior resembles that of the shear modulus⁹ and suggests that the TO frequency changes may have an elastic origin. Although the resonant frequency of a torsional oscillator containing solid helium depends primarily on the oscillator's total moment of inertia, it is also affected by the helium's elastic response. An increase in the elastic stiffness of any part of an oscillator, e.g., in the solid helium's shear

modulus, will raise the oscillator's frequency and mimic decoupling. However, simple estimates and detailed numerical modeling of typical TO geometries¹² show that a 30% modulus change in the solid ^4He would produce TO frequency changes much smaller than those attributed to decoupling so changes in the helium's stiffness do not appear to be sufficient to explain the observed NCRI.

There are a number of other observations that are difficult to reconcile with an elastic origin of the TO behavior. Solid helium grown in the pores of Vycor glass shows essentially the same TO NCRI as bulk helium but ultrasonic measurements¹³ do not show elastic changes like those in bulk helium. Also, shear modulus and TO measurements showed different behavior in solid ^3He .¹⁴ The temperature and amplitude dependence of the shear modulus of hcp ^3He were essentially the same as in hcp ^4He , as expected if dislocation motion and impurity pinning are responsible for the modulus changes. However, in contrast to the behavior with ^4He , in ^3He the TO frequency did not increase at low temperature—NCRI appears to be associated only with the Bose solid. Recent TO oscillator measurements¹⁵ also show that the critical stress for amplitude dependence in TO experiments is much lower than the critical stress for the shear modulus anomaly. Finally, recent TO measurements¹⁶ show an NCRI that depends on the DC rotation rate, something very difficult to reconcile with a nonsupersolid origin.

In an attempt to increase defect densities and enhance the NCRI, Mulders *et al.*¹⁷ grew ^4He crystals in a 95% porosity silica aerogel. Aerogels have an open structure with a wide range of pore sizes, which can be characterized by a fractal distribution with cutoffs at small lengths (the silica strand size, around 3 nm) and at large lengths (maximum pore size, around 100 nm for 95% porosity). X-ray diffraction measurements showed that the ^4He crystals grown in the aerogel were highly polycrystalline (crystallite size ~ 100 nm) and so contained many grain boundaries or other defects. However, the TO measurements on crystals grown in aerogel showed very small NCRI (0.04%) with a low onset temperature (~ 100 mK). This is typical of the behavior seen in high quality single crystals of bulk ^4He , rather than what was expected in a highly disordered crystal. It also contrasts with the large NCRI (several percent) and higher onset temperatures (~ 200 mK) seen in denser porous media like Vycor glass.¹⁸

The elastic behavior of solid helium also should be strongly affected by confinement in an aerogel. Dislocation densities could be larger but the dislocations would not be mobile. The pinning of dislocations by ^3He impurities in bulk ^4He is attributed to the volume mismatch between impurity and lattice atoms. This produces, for example, an interaction with the strain field around an edge dislocation, attracting it with a binding energy of order 1 K for ^4He .^{10,19,20} The interaction between dislocations and silica strands would be much stronger, pinning them very effectively. The density of silica strands in a 95% porosity aerogel is about $10^{11}/\text{cm}^2$ and the corresponding mean free path (average straight-line distance before meeting a strand) is about 50 nm. This puts an upper limit on the pinning length of dislocations that is much shorter than the typical loop lengths inferred from ultrasonic measurements in solid helium ($\sim 5 \mu\text{m}$), which means that dislocations should have only small effects on the shear

modulus of solid helium in aerogel. If dislocations unbind from the silica strands, it would happen at higher temperatures and stresses than in bulk helium.

In order to clarify the relationship between defects, particularly mobile dislocations, and the observed TO and elastic anomalies, we have made shear modulus measurements on solid ^4He crystals grown in the pores of an aerogel. At temperatures above 100 mK we observe new behavior—a large, gradual modulus decrease that extends all the way to melting, accompanied by a broad dissipation peak. This behavior is independent of amplitude and its frequency dependence is consistent with a thermal relaxation process with a broad range of activation energies centered around 16 K. We interpret this behavior in terms of stress relaxation via vacancy diffusion, either directly or through climb of dislocations. Below 100 mK, we see a small modulus and dissipation anomaly much like that seen in bulk ^4He , including its amplitude dependence. Although this could be due to solid helium in the aerogel pores, it may simply reflect elastic changes in the bulk ^4He surrounding the aerogel sample and transducers.

II. EXPERIMENTAL DETAILS

For these experiments, we used an aerogel similar to those used in the x-ray and TO experiments.¹⁷ It was grown using a single step, base catalyzed process with a final porosity of 95%. We cut a thin slice (thickness $D = 0.8$ mm) from the aerogel (a cylinder of diameter 12.5 mm). The aerogel slice was placed in the gap between two parallel piezoelectric shear transducers, which were adjusted to slightly compress it (see Fig. 1). After mounting the aerogel, the whole arrangement was sealed into a copper cell (volume ~ 20 cm³), which included a capacitive gauge to measure the pressure in situ. The cell was attached to the mixing chamber of a dilution refrigerator. Temperatures were measured with a calibrated germanium sensor, supplemented by a ^{60}Co nuclear orientation thermometer at temperatures below 50 mK. Crystals were grown from ^4He (0.3 ppm ^3He) over a period of about 10 hours (using the blocked capillary technique), filling the aerogel and surrounding volume with solid helium. Although the aerogel slice covered the transducer faces and filled the gap, its surfaces were not perfectly flat, leaving small gaps between the aerogel and the transducers which were filled with solid helium. The edges of the transducers and aerogel were also in contact with bulk helium.

The elastic measurements were made on the aerogel/helium system in the same way as in our previous experiments⁸ on

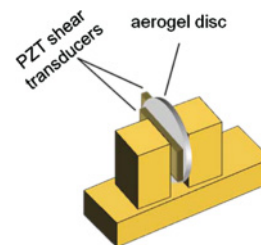


FIG. 1. (Color online) An aerogel disk in the 0.8-mm gap between two parallel piezoelectric shear transducers, as described in the text.

bulk ^4He and ^3He . An ac voltage V with angular frequency $\omega = 2\pi f$, was applied to one transducer (with width $W = 9.7$ mm, length $L = 12.8$ mm, overlap area $A = 1$ cm 2 , and piezoelectric coefficient d_{15}), generating a shear displacement $\delta x = d_{15}V$ at its surface, a strain $\epsilon = \delta x/D$ in the helium-filled aerogel and a stress σ on the detecting transducer. This produced a charge q which was measured as a current $I = \omega q$, giving the shear modulus as $\mu = \frac{\sigma}{\epsilon} = \left(\frac{D}{2\pi d_{15}A}\right)\left(\frac{I}{fV}\right)$. For purely elastic deformations, the stress is in phase with the applied strain but, in general, the stress lags the strain by a phase angle ϕ , which is related to the dissipation by $1/Q = \tan \phi$ ($\approx \phi$ for small dissipation). The amplitude and phase of the current thus give the real and imaginary parts of the helium's shear modulus, although electronic phase shifts prevented us from measuring absolute values of $1/Q$. The data were corrected for a background signal due to electrical crosstalk, determined using measurements with liquid helium in the cell. The modulus and dissipation were measured at frequencies between 2 and 2000 Hz, a range limited by signal to noise at the low end and by the presence of an acoustic resonance at 4500 Hz.

The elastic constants of high porosity silica aerogels are very small. We measured²¹ the bulk modulus of the 95% aerogel used in these experiments as $K = 0.43$ MPa. The shear modulus of aerogels is typically about 25% smaller than the bulk modulus so we estimate a shear modulus of about 0.3 MPa for this sample, comparable to values found in other aerogels with similar density.²² This is only about 2% of the shear modulus of solid ^4He at pressures around 35 bar. This means that the total shear modulus we measure is dominated by the modulus of the solid helium in the pores with only a small contribution from the aerogel itself.

III. RESULTS

Figure 2 shows the temperature dependence of the shear modulus μ/μ_o and of the dissipation $1/Q$ at a frequency of 2000 Hz, for two solid ^4He samples grown in the aerogel. The moduli are normalized by their values at the lowest temperature and the absolute values of the phase shifts cannot be accurately determined in our measurements so the data are really changes in dissipation. Sample 1 has a pressure 29.7 bar and melts at 1.77 K (the hcp/bcc/liquid triple point). Sample 2 has a pressure 35.9 bar and melts at 1.95 K. The higher pressure sample has a slightly larger modulus at low temperatures but the two samples' temperature dependencies are similar. Their shear moduli decrease with temperature by about 50% at the melting temperature. These modulus changes are accompanied by broad dissipation peaks around 0.7 K, near the midpoints of the modulus changes. For comparison, we also show data (shifted vertically for clarity) at the same frequency from a typical bulk helium crystal (33.3 bar, 0.3 ppm ^3He) grown using the blocked capillary method. The behavior of the two samples grown in aerogel is strikingly different from that of the bulk sample. The total modulus changes in the aerogel are much larger (about 50%) than in the bulk sample (about 8%). In aerogel, the modulus decrease occurs gradually over the entire temperature range up to melting while in bulk helium it occurs entirely below 200 mK. The dissipation peaks in the aerogel

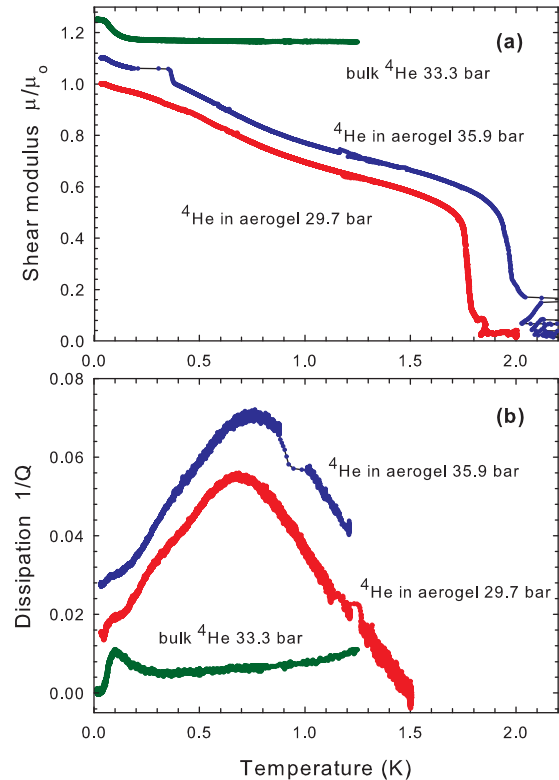


FIG. 2. (Color online) Temperature dependence of (a) shear modulus and (b) dissipation for ^4He crystals at 29.7 and 35.9 bar in aerogel, compared to a bulk ^4He crystal at 33.3 bar.

sample are also larger and broader than the corresponding peak in bulk helium, as well as occurring at higher temperature (around 0.7 K, compared to 110 mK for the the bulk peak).

The magnitudes of the total modulus change and the heights of the dissipation peaks are independent of the measurement frequency but their temperature dependence is not. Figure 3 shows the behavior for the 29.7 bar sample in aerogel at frequencies from 2 to 2000 Hz. The modulus changes and dissipation peaks shift to lower temperatures as the frequency decreases. This behavior is characteristic of a thermally activated relaxation process. For a simple Debye process with a relaxation time τ , the modulus μ and dissipation $1/Q$ are related to the real and imaginary parts of the shear modulus:²³

$$\frac{\mu}{\mu_o} = 1 - \frac{\delta\mu}{\mu_o} \frac{1}{1 + (\omega\tau)^2}, \quad (1)$$

$$\frac{1}{Q} = \frac{\delta\mu}{\mu_o} \frac{\omega\tau}{1 + (\omega\tau)^2}, \quad (2)$$

where μ_o is the “unrelaxed modulus” ($\omega\tau \gg 1$) and $\mu_o - \delta\mu$ is the “relaxed modulus” ($\omega\tau \ll 1$). The strength of the relaxation determines the total change $\delta\mu/\mu_o$. For the samples confined in aerogel, the modulus changes up to melting, shown in Fig. 2, correspond to $\delta\mu/\mu_o \sim 0.5$, while the modulus change seen at lower temperature in the bulk sample corresponds to $\delta\mu/\mu_o \sim 0.08$. For a thermally activated process with a single activation energy E , $\tau(E) = \tau_o e^{\frac{E}{kT}}$. The crossover from unrelaxed to relaxed modulus occurs at the temperature where $\omega\tau = 1$. At this point the dissipation is maximum and 50% of the modulus change has occurred. These points (indicated

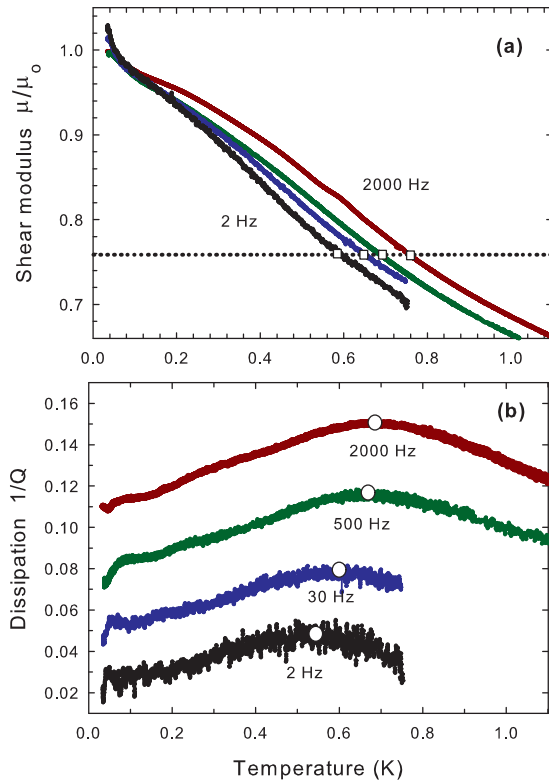


FIG. 3. (Color online) Frequency dependence of (a) the modulus and (b) the dissipation for the 29.7 bar crystal of Fig. 2. Squares mark the points at which 50% of the modulus change has occurred and the circles mark the positions of the corresponding dissipation peaks.

by circles and squares in Figs. 3(b) and 3(a) can be used to determine the temperature dependence of τ .

Figure 4 is an Arrhenius plot ($1/T$ versus $\ln f$) of the crossover temperatures marked on Fig. 3. The dissipation peak temperatures (circles) were determined by fitting the curves in Fig. 3(b). The line is a best fit to these peak temperatures, giving an activation energy $E = 15.9 \pm 5$ K. The large error bars (and resulting large uncertainty in E) reflect the difficulty

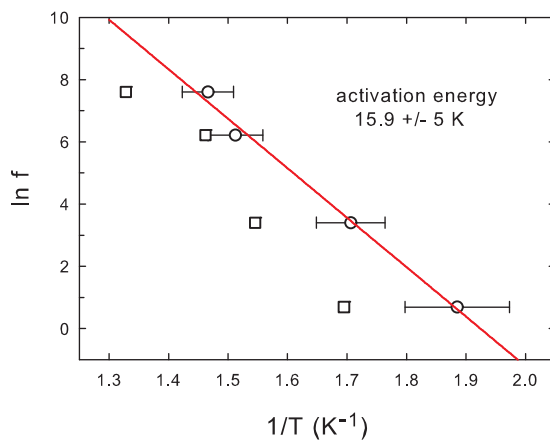


FIG. 4. (Color online) Thermal activation of elastic relaxation for 29.7-bar helium crystal in aerogel. Circles are the dissipation peaks; squares are the modulus points shown in Fig. 3. The line is a least squares fit to the dissipation peak data, giving an activation energy of 15.9 K.

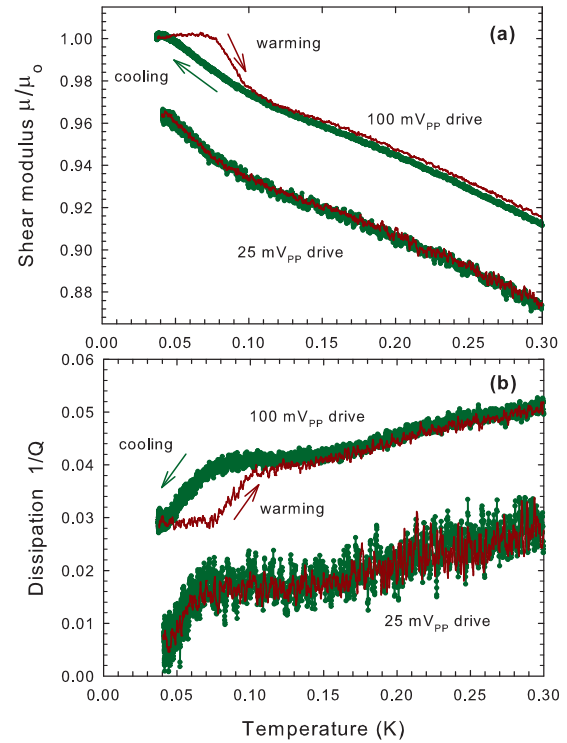


FIG. 5. (Color online) (a) Normalized shear modulus and (b) dissipation. The upper curves in each panel are data taken at a drive voltage of 100 mV_{pp} and show hysteresis between cooling and warming. The lower curves (which have been vertically shifted for clarity) were taken at lower drive voltage (25 mV_{pp}) and show no hysteresis.

in locating the maxima of such broad dissipation peaks, given the noise in the data.

Figure 5 presents data taken at 500 Hz during thermal cycling, showing a small hysteresis loop below 100 mK. The hysteresis between cooling and warming disappeared when the drive voltage was reduced from 100 to 25 mV_{pp}. The amplitude dependence in this temperature range is characteristic of the modulus anomaly seen in bulk helium so we examined it in more detail. Figure 6(a) shows the modulus (measured during cooling) for a series of drive voltages ranging from 25 to 8000 mV_{pp}. Figure 6(b) shows the corresponding dissipation data from 100 to 8000 mV_{pp} (the 25 mV_{pp} data were too noisy to be useful). No amplitude dependence was seen above 300 mK and the curves have been shifted vertically to agree at high temperatures. The modulus and dissipation at low temperature (below 150 mK) were, however, reduced when the sample was cooled at high drive amplitudes.

The amplitude dependence was further studied by varying the drive amplitude at low temperatures. Figure 7 shows the resulting hysteretic behavior at the base temperature of the fridge, 25 (circles) and at 50 mK (squares). The sample was initially cooled at the highest drive amplitude (8000 mV). When the drive was then reduced at low temperature, the modulus increased (open circles), as would be expected based on Fig. 6(a). However, when the drive was subsequently raised (solid symbols), the modulus was higher than during lowering the drive amplitude. At 25 mK, it remained at its largest value right up to the highest drive voltage. At 50 mK it

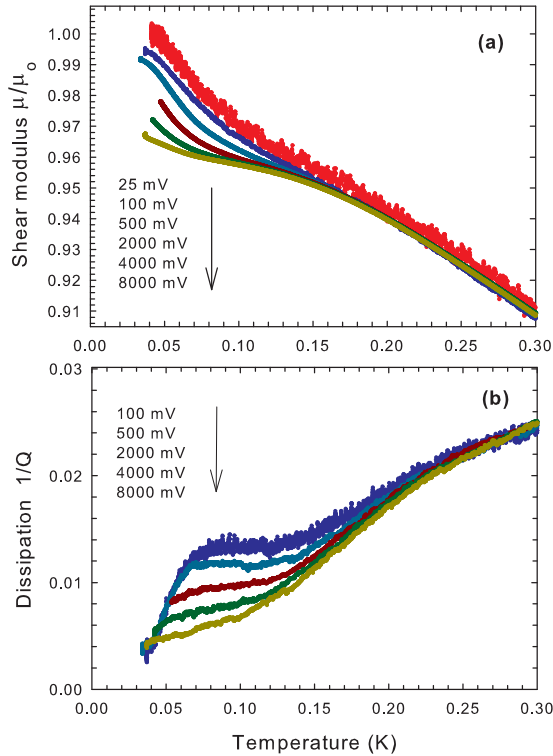


FIG. 6. (Color online) (a) Normalized shear modulus and (b) dissipation in a 29.7-bar ⁴He crystal in aerogel as a function of drive voltage. Below 150 mK, the modulus and dissipation decrease as the amplitude increases.

decreased for larger drive amplitudes so the hysteresis was much smaller. At higher temperatures we saw no amplitude-dependent hysteresis.

The small low-temperature anomaly seen in the modulus and dissipation below 150 mK has essentially the same dependence on temperature and amplitude, including hysteresis, as is seen in bulk helium crystals. However, the modulus change (about 4%) is smaller than that in bulk helium (where it ranges from about 7 to 30%), as is the associated low-temperature dissipation.

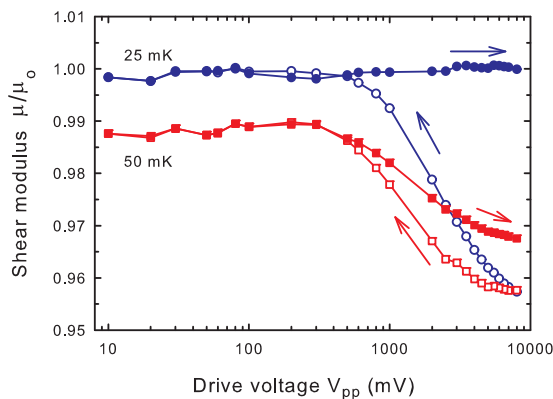


FIG. 7. (Color online) Hysteresis in amplitude dependence for a 29.7-bar crystal in aerogel. Data have been corrected for small variations in the gain of the preamplifier using data at 400 mK where there is no amplitude dependence or hysteresis.

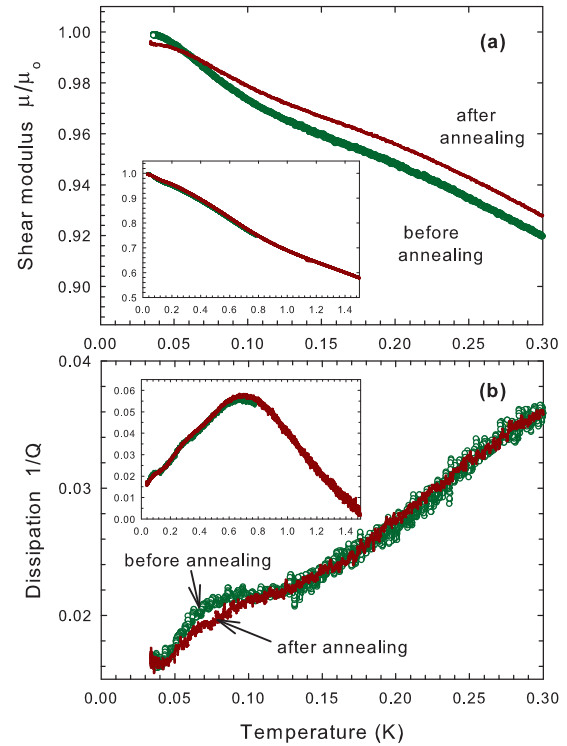


FIG. 8. (Color online) (a) Normalized modulus and (b) dissipation at low temperatures in a 29.7-bar crystal in aerogel, before and after annealing at 1.5 K. The insets show the same data over a wider temperature range.

Finally, we looked at the effect of annealing on the modulus and dissipation. Figure 8 shows the modulus and dissipation at 2000 Hz during cooling, before and after annealing the sample at 1.5 K (0.2 K below the hcp/bcc transition) for 17 hours. The low-temperature anomaly was changed by annealing—both the modulus change and the dissipation were reduced below 150 mK, as was the amplitude-dependent hysteresis. This is similar to the annealing behavior seen in bulk helium crystals.⁹ The temperature dependence above 150 mK, on the other hand, was essentially unaffected by annealing, as shown in the insets in Fig. 8. The dissipation peak’s magnitude and position were essentially unchanged and the modulus shifted uniformly upward by about 1.4%.

IV. DISCUSSION

These measurements of the shear modulus and dissipation in solid ⁴He confined in aerogel show distinctly different behavior above and below 150 mK. The low-temperature behavior resembles that in bulk helium crystals, although the magnitude of the modulus and dissipation anomaly is smaller. The high-temperature behavior is quite different. The changes in modulus and dissipation are larger than in bulk helium, occur at much higher temperature, and over a broader temperature range.

The torsional oscillator experiments with aerogel¹⁷ showed a small NCRI at temperatures below 100 mK, behavior more typical of single crystals than of highly disordered helium. Our elastic measurements also show small, bulklike effects below 100 mK. Unfortunately, it is not possible in our experiments

to distinguish low-temperature behavior occurring inside the aerogel from similar bulk effects in the helium surrounding the aerogel and transducers. The elastic strain generated by the driving transducer does not stop at the edge of the gap containing the aerogel but extends into the surrounding bulk helium and generates a force on the receiving transducer. At the relatively low frequencies of these measurements, the bulk stress is in phase with that in the aerogel in the gap and the two signals add. The magnitude of the bulk helium contribution to the measured signal can be estimated from the transducer dimensions. At the edge of the transducers, the bulk strain is equal to that in the gap but it drops off over a length scale of order of the gap thickness D . The volume of the bulk region, which is elastically strained is roughly the square of this distance ($D = 0.8$ mm) multiplied by the perimeter of the gap ($2W + 2L = 45$ mm). The fraction of the measured transducer current coming from the bulk solid is $\frac{I_{\text{bulk}}}{I_{\text{aerogel}}} \lesssim \frac{V_{\text{bulk}}}{V_{\text{aerogel}}} = \frac{D^2(2W+2L)}{DWL} \approx 0.36$, i.e., the surrounding bulk helium contributes as much as 36% to the measured modulus, so an 11% stiffening in the bulk helium could produce the observed 4% modulus change at low temperatures. It is difficult to estimate this contribution more accurately since the stiffening seen in bulk varies from about 7 to 30%. Also, if only the C_{44} elastic constant changes (as expected if dislocation motion is responsible for the stiffening²⁴), the bulk contribution will depend strongly on the unknown orientation of the bulk crystallites at the transducer edges.

Given these uncertainties, it is plausible that the low-temperature modulus changes seen in Figs. 5 to 8 are entirely due to bulk helium in the cell. However, they could be a contribution from bulklike behavior in solid helium in the aerogel pores, analogous to the period changes in the TO observations. The only way to be sure would be to eliminate all bulk helium around the transducers by growing the aerogel around them. However, the high-temperature supercritical drying required to make aerogels would destroy the piezoelectric poling of our transducers. Although there are other transducer materials that do not depole at these temperatures but they have much smaller piezoelectric coefficients than PZT, which would make low-amplitude measurements very difficult.

In contrast to the anomaly below 150 mK, the behavior at higher temperatures is quite different from that of bulk helium and is clearly associated with the helium confined in the aerogel. We will focus on this regime in the following discussion. It is clear from Fig. 2 that the total modulus change is much larger in the aerogel than in bulk ^4He and that it occurs over a wider temperature range, extending all the way to the melting point. As the frequency dependence of Figs. 3 and 4 shows, this modulus decrease and the accompanying dissipation peak are associated with a thermally activated process. This is also true in bulk ^4He ¹⁰ but the activation energy is much larger in aerogel (about 16 versus 0.7 K in bulk). If, as in bulk helium, the modulus drop in aerogel is due to unpinning of dislocations whose motion then weakens the crystal, the larger activation energy, and the resulting higher temperature at which the changes occur, could reflect the much stronger pinning of dislocations by aerogel strands than by ^3He impurities. However, as for bulk helium, the dissipation peaks and modulus crossover in aerogel are not consistent with a simple Debye relaxation. For a relaxation

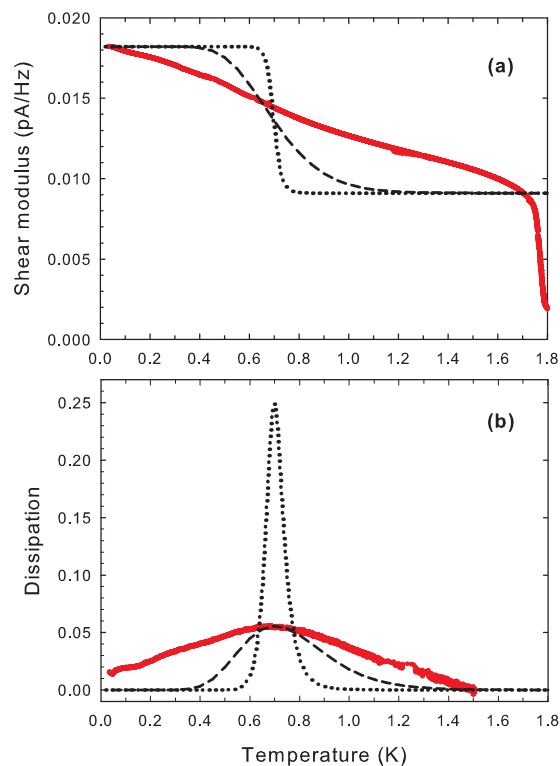


FIG. 9. (Color online) Debye relaxation fits for the shear modulus and dissipation. Red points are 2000-Hz data from Fig. 2, dotted lines are fits with a single activation energy (15.9 K), and dashed line is a fit with a log normal distribution of activation energies, as described in the text.

process with a single activation energy, the total modulus change and the height of the dissipation peak are directly related by $(1/Q)_{\text{peak}} = \delta\mu/2\mu_0$. This would give dissipation peaks of magnitude $1/Q \sim 0.25$ and ~ 0.045 for the confined and bulk samples of Fig. 2, respectively, but the observed dissipation peaks are about 4 times smaller, roughly 0.06 and 0.01. Figure 9 compares the 2000-Hz data to the Debye relaxation predictions for a single activation energy (the dotted lines are for $E = 15.9$ K, $\tau_0 = 10^{-14}$ s).

In addition to the discrepancy between the predicted and observed dissipation peak heights, the modulus crossover and the dissipation peak in aerogel are also much broader than predicted for a single activation energy. These discrepancies suggest that the relaxation, although thermally activated, involves a distribution of activation energies that broadens the crossover and reduces the height of the dissipation peak. For bulk helium, a detailed analysis of the temperature and frequency dependence of the low-temperature modulus and dissipation anomaly showed¹⁰ that it could be described by a log normal distribution of activation energies

$$n(E) = B e^{-\frac{(\ln E - \ln \Delta)^2}{w^2}}, \quad (3)$$

where B is a normalization factor and Δ is the characteristic activation energy. This distribution has a long tail at large E and approaches zero for small E . The modulus and dissipation are found by multiplying $n(E)$ by the contributions from Eqs. (1) and (2) and integrating over all energies E . In a sample similar

to the bulk crystal of Fig. 2, the data were fit reasonably well¹⁰ using an average value $\Delta = 0.73$ K and a width $W = 0.45$.

We can try to fit the modulus and dissipation in solid helium in aerogel using such a distribution. The dashed (blue) line in Fig. 9 shows such a calculation for $E = 15.9$ K, $\tau_o = 3 \times 10^{-15}$ s, and $W = 0.3$. The values of τ_o and W were chosen to match the temperature and height of the dissipation peak. However, this distribution does not give a good fit to the aerogel data—the actual broadening is substantially larger and the roughly linear decrease of the modulus with temperature is not reproduced, suggesting that the actual distribution must have more weight at low energy. Using an even wider distribution of activation energies would further broaden the transition but would also predict a smaller dissipation peak. Also, the attempt time τ_o is about two orders of magnitude shorter than solid helium's inverse Debye frequency, which seems unphysical.

Previous ultrasonic measurements have probed the elastic moduli of solid helium confined in the pores of a dense (87% porosity) aerogel²⁵ and of Vycor.²⁶ The speed of longitudinal sound waves in an isotropic solid is given by $\sqrt{(K + 4\mu/3)/\rho}$, i.e., the bulk modulus K and the shear modulus μ contribute almost equally to the sound speed. In a porous medium, the distinction between transverse and longitudinal sound is even less significant since the deformation at the pore scale is inhomogeneous and involves both shear and compressional strains. Figure 10 shows the effective longitudinal modulus ($K + 4\mu/3$) and the corresponding dissipation at 9 MHz (determined from the measured velocity and attenuation of longitudinal ultrasound) in the aerogel for a ⁴He crystal at pressure of 48 bar. The shear and bulk moduli of this aerogel are approximately 47 and 67 MPa,²⁷ about 150 times larger than those of the 95% aerogel studied in this paper and three times larger than the corresponding moduli of solid ⁴He. When the helium freezes (around 2.1 K) the longitudinal modulus increases by about 25%, i.e., by 32 MPa. This is comparable to the contribution expected from the added shear modulus of the solid helium in the pores, $4\mu_{\text{He}}/3 \approx 25$ MPa.²⁸ As in our modulus measurements with the 95% aerogel, the change is gradual, occurring between freezing and the lowest temperature (200 mK). The modulus change is accompanied by a dissipation peak around 1.75 K. This is substantially higher than the temperatures of the dissipation peaks in Figs. 2 and 3, as expected for an activated process, given the much higher frequency in the ultrasonic measurement. However, the two aerogels are quite different and so their behaviors cannot be directly compared. Also, the large ultrasonic attenuation in this aerogel did not allow measurements at higher frequencies so it was not possible to confirm directly that the observed modulus and dissipation could be described by a thermally activated process.

Similar measurements have been made with porous Vycor glass^{26,29} using transverse ultrasound. Figure 11 shows the shear modulus and dissipation from transverse sound velocity and attenuation measurements at 16 MHz. At this pressure (62 bar) the ⁴He in the pores freezes at 1.94 K. Again, the modulus change due to the solid ⁴He occurs gradually over a wide temperature range and is accompanied by a broad dissipation peak. Vycor has a smaller porosity (29%) and a much higher shear modulus (7.5 GPa) than the aerogels, so the fractional modulus change due to freezing of helium

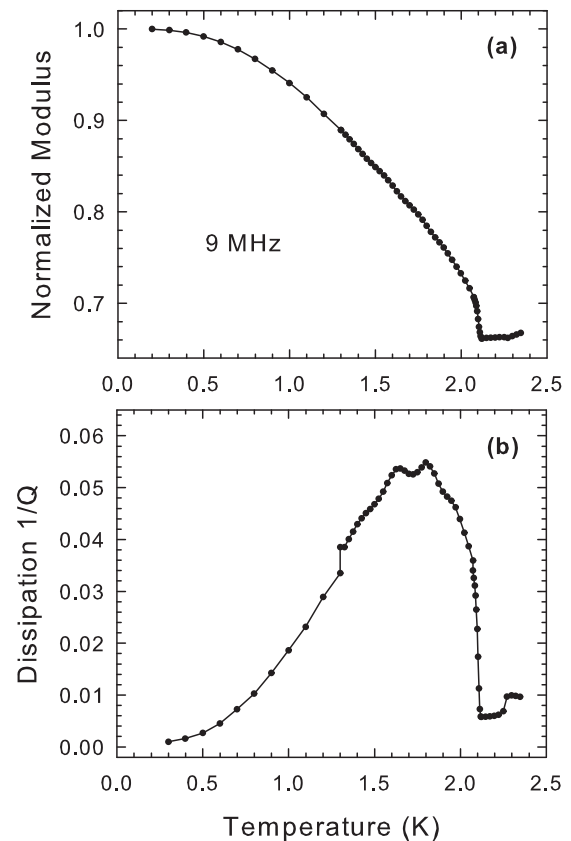


FIG. 10. (a) longitudinal modulus $K + 4\mu/3$ (normalized by its low-temperature value) in a solid helium-filled dense aerogel (87% porosity) aerogel measured at 9 MHz using longitudinal ultrasonic waves²⁵ (b) dissipation determined from the attenuation of the same ultrasonic waves.

in its pores is smaller (less than 1%), as is the associated dissipation peak. In this case, ultrasonic measurements were made at frequencies from 8 to 30 MHz, allowing an activation energy for the responsible process to be determined. The value was 14 K, similar to the 16 K activation energy from Fig. 4. However, the ultrasonic velocity and attenuation changes were interpreted in terms of stress relaxation through a creep process involving vacancy diffusion, rather than the motion of dislocations (which cannot exist as well-defined bulklike defects in the 3.5-nm-radius pores of Vycor). The time constant for such a diffusive process goes as the square of the pore size and so is very short in Vycor (about 1 ns at melting), allowing stress relaxation on ultrasonic time scales.

Aerogels have about 10^{11} silica strands/cm², with a diameter of about 3 nm. These should provide very effective pinning sites for dislocations in the solid helium so we expect them to be pinned on a length scale comparable to the mean free path in the aerogel, about 50 nm. This is much shorter than the typical dislocation loop lengths inferred from ultrasonic measurements in solid helium ($L \sim 5 \mu\text{m}$) meaning that dislocations should be almost completely pinned and so should have only small effects on the shear modulus of the helium. For $L = 50$ nm, ΛL^2 would be only 0.025 even for a very high dislocation density ($\Lambda = 10^9 \text{ cm}^{-2}$) and negligible for dislocation densities $\Lambda = 10^6 \text{ cm}^{-2}$ characteristic of single crystals. Since the interaction of a dislocation with

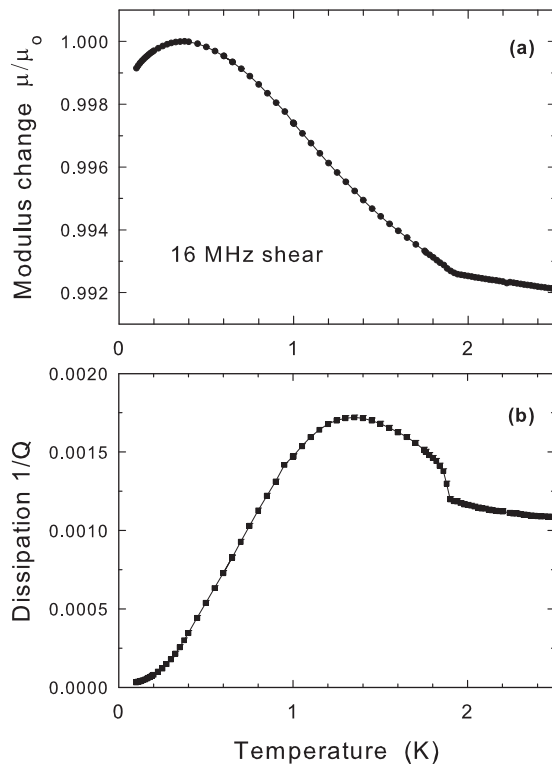


FIG. 11. Shear modulus and dissipation in solid helium-filled Vycor glass, measured at 16 MHz using transverse ultrasonic waves.²⁶

an aerogel strand will be much stronger than with a ^3He impurity in bulk ^4He , thermal unbinding of dislocations from pinning sites would occur at higher temperatures than in bulk and stress-induced unpinning would require very large stress amplitudes. The disordered aerogel structure would not give a single pinning energy and so would give a broad crossover as the crystal is warmed.

From the frequency dependence of the modulus and dissipation for ^4He in aerogel, it is clear that a process with a thermal activation energy of about 16 K is involved. This is comparable to the activation energy for vacancy motion in helium from NMR and other measurements³⁰ (which range from about 8 to 16 K at pressures near melting) and from

recent computations³¹ (13 K at the melting density). Vacancy activation energies in bulk ^4He depend on molar volume but over our limited pressure range (29.7 to 35.9 bar) the variation is only about 10%, much smaller than the uncertainty in our measurements or the scatter in the experimental values in bulk helium.³⁰ Stress relaxation via direct vacancy diffusion would be much slower than in Vycor, due to the larger pore size in aerogels, but could occur at the low frequencies used in our shear modulus measurements. Diffusion can also relax stresses indirectly, by allowing dislocations to climb (move perpendicular to their Burgers vectors). This requires mass transport to/from the dislocation and so normally occurs only at high temperatures where thermally activated vacancies are available. In solid helium, where the cores of some dislocations may be superfluid,⁶ mass could also be transported along the dislocation core, allowing “superclimb”³² at low temperatures. This would not require thermal activation and so does not appear to be responsible for the behavior we observe.

Whatever specific relaxation mechanism is responsible for the high-temperature modulus relaxation we observe in aerogels, the large changes have implications for torsional oscillator measurements. If, as has been suggested,⁵ the apparent NCRI in TO measurements really has its origin in elastic changes in the solid helium, then the 50% modulus change we observe at high temperatures should be much more important than the relatively small changes below 150 mK, even if those are occurring within the aerogel. The modulus changes would appear as a smooth “background” temperature dependence above 150 mK. The published data¹⁷ do not appear to show such a background, but only extend to 300 mK. Note that a similar background might be expected in TO experiments with solid helium in Vycor, since the modulus change due to freezing (~ 56 MPa) is even larger than that in aerogels (even though the fractional modulus change is much smaller).

ACKNOWLEDGMENTS

This work was supported by NSERC Canada. We would like to acknowledge valuable conversations with M. H. W. Chan and N. Mulders.

¹E. Kim and M. H. W. Chan, *Science* **305**, 1941 (2004).

²S. Balibar and F. Caupin, *J. Phys. Condens. Matter* **20**, 173201 (2008).

³A. S. C. Rittner and J. D. Reppy, *Phys. Rev. Lett.* **97**, 165301 (2006).

⁴A. S. C. Rittner and J. D. Reppy, *Phys. Rev. Lett.* **98**, 175302 (2007).

⁵J. D. Reppy, *Phys. Rev. Lett.* **104**, 255301 (2010).

⁶M. Boninsegni, A. B. Kuklov, L. Pollet, N. V. Prokof'ev, B. V. Svistunov, and M. Troyer, *Phys. Rev. Lett.* **99**, 035301 (2007).

⁷L. Pollet, M. Boninsegni, A. B. Kuklov, N. V. Prokof'ev, B. V. Svistunov, and M. Troyer, *Phys. Rev. Lett.* **98**, 135301 (2007).

⁸J. Day and J. Beamish, *Nature (London)* **450**, 853 (2007).

⁹J. Day, O. Syshchenko, and J. Beamish, *Phys. Rev. B* **79**, 214524 (2009).

¹⁰O. Syshchenko, J. Day, and J. Beamish, *Phys. Rev. Lett.* **104**, 195301 (2010).

¹¹P. Gumann, D. Ruffner, M. Keiderling, and H. Kojima, *J. Low Temp. Phys.* **158**, 577 (2010).

¹²A. C. Clark, J. D. Maynard, and M. H. W. Chan, *Phys. Rev. B* **77**, 184513 (2008).

¹³T. Kobayashi, S. Fukuzawa, J. Taniguchi, M. Suzuki, and K. Shirahama, *AIP Conf. Proc.* **850**, 333 (2006).

¹⁴J. T. West, O. Syshchenko, J. Beamish, and M. H. W. Chan, *Nat. Phys.* **5**, 598 (2009).

¹⁵D. Y. Kim, H. Choi, W. Choi, S. Kwon, E. Kim, and H. C. Kim, *Phys. Rev. B* **83**, 052503 (2011).

¹⁶H. Choi, D. Takahashi, K. Kono, and E. Kim, *Science* **330**, 1512 (2010).

- ¹⁷N. Mulders, J. T. West, M. H. W. Chan, C. N. Kodituwakku, C. A. Burns, and L. B. Lurio, *Phys. Rev. Lett.* **101**, 165303 (2008).
- ¹⁸E. Kim and M. H. W. Chan, *Nature (London)* **427**, 225 (2004).
- ¹⁹I. Iwasa and H. Suzuki, *J. Phys. Soc. Jpn.* **49**, 1722 (1980).
- ²⁰M. A. Paalanen, D. J. Bishop, and H. W. Dail, *Phys. Rev. Lett.* **46**, 664 (1981).
- ²¹T. Herman, J. Day, and J. Beamish, *Phys. Rev. B* **73**, 094127 (2006).
- ²²D. R. Daughton, J. MacDonald, and N. Mulders, *J. Non-Cryst. Solids* **319**, 297 (2003).
- ²³A. S. Nowick and B. S. Berry, *Anelastic Relaxation in Crystalline Solids* (Academic Press, New York, 1972).
- ²⁴X. Rojas, A. Haziot, V. Babst, S. Balibar, and H. J. Maris, *Phys. Rev. Lett.* **105**, 145302 (2010).
- ²⁵E. B. Molz and J. R. Beamish, *J. Low Temp. Phys.* **101**, 1055 (1995).
- ²⁶J. R. Beamish, N. Mulders, A. Hikata, and C. Elbaum, *Phys. Rev. B* **44**, 9314 (1991).
- ²⁷Y. Xie and J. R. Beamish, *Phys. Rev. B* **57**, 3406 (1998).
- ²⁸D. S. Greywall, *Phys. Rev. B* **3**, 2106 (1971).
- ²⁹Vycor 7930 Porous Glass manufactured by Corning Incorporated.
- ³⁰B. A. Fraass, P. R. Granfors, and R. O. Simmons, *Phys. Rev. B* **39**, 124 (1989).
- ³¹M. Boninsegni, A. B. Kuklov, L. Pollet, N. V. Prokof'ev, B. V. Svistunov, and M. Troyer, *Phys. Rev. Lett.* **97**, 080401 (2006).
- ³²S. G. Soyler, A. B. Kuklov, L. Pollet, N. V. Prokof'ev, and B. V. Svistunov, *Phys. Rev. Lett.* **103**, 175301 (2009).